JOURNAL OF MATERIALS SCIENCE 30 (1995) 3761–3767

Three-dimensional analysis of modulated photoreflectance in a silicon wafer

H. C. KIM, SUN CHUL KIM, MOON GYU JANG, JEONG KI LEE
Department of Physics, Korea Advanced Institute of Science and Technology, 373-1 Gusong-dong, Yusong-gu, Taejon 305-701, Korea

The effects of probe and pumping beam size and modulation frequency on photoreflectance were investigated for a silicon wafer by considering one- and three-dimensional generation and propagation of thermal and plasma waves, PR_{1D} and PR_{3D}. The magnitude of PR_{1D} decreased as the inverse square of the effective beam radius and that of PR_{3D} was 100 times smaller than PR_{1D} at 0.1 μm effective beam radius and decreased with the effective beam radius. The phase shift of PR_{1D} was nearly constant at 225°, whereas that of PR_{3D} increased with the effective beam radius from 0° to 225°. The magnitude and phase of PR_{3D} become the same as those of PR_{1D} by satisfying the equivalence conditions, where the probe and pumping beam radii are larger than the thermal and plasma wavelengths, when the effective beam radius was larger than 112 μm. PR_{1D} decreased with modulation frequency as $\omega^{-1/2}$, whereas the magnitude of PR_{3D} was nearly constant and 100 times smaller than that of PR_{1D} at 1 kHz modulation frequency. The PR_{1D} phase varied from 180° to 225°, but that of the PR_{3D} increased from 0° to that of PR_{1D} with increase of the modulation frequency. As the modulation frequency increased, the magnitude and phase of PR_{3D} approached to those of PR_{1D} by approaching the equivalence conditions, owing to the decrease of the thermal and plasma wavelengths. The good agreements in the modulation frequency dependence of the magnitude and phase of PR_{3D} with those measured, justified the three-dimensional analysis of the photoreflectance.

1. Introduction

Optical properties can be altered by the absorption of incident energy when a material is excited with an intensity-modulated pumping beam. This results in a change of the sample's complex refractive index, undergoing periodic variations at the modulation frequency of the pumping beam, and the induced changes can be detected by measuring the modulated reflectance of the probe beam from the sample surface. In most materials, the modulated photoreflectance signal arises purely from a temperature variation [1, 2], because the optical properties of most materials are dependent on the sample temperature. The temperature of the sample surface varies with the modulation frequency of the pumping beam and the reflectance of the probe beam experiences a corresponding modulation. In a semiconductor, however, there are often more significant contributions to the photoreflectance signal arising from the free carriers generated by the pumping beam. The photo-excited electron–hole plasma effects, including the thermal effects, are associated with free-carriers recombination [3], a free-carrier Drude effect [4, 5] on the optical refractive index.

The probe and pumping beam radii and the modulation frequency of the pumping beam are the important parameters which determine the generation and propagation of thermal and plasma waves. The probe and pumping beam radii, in the one-dimensional consideration, are assumed to be much larger compared to the wavelengths of thermal and plasma waves which are determined from the modulation frequency. The magnitude of the photoreflectance varies as $\omega^{-1/2}$ with the modulation frequency, whereas the phase has a constant value [6–8]. When the probe and pumping beam radii are sufficiently larger than the wavelengths of thermal and plasma waves, the experimentally measured magnitude and phase of PR have the same dependence as those of the one-dimensional calculation [7, 8]. However, in most cases, the probe and pumping beam radii are ~ 1 μm, and the thermal and plasma wavelengths are about 40–100 μm at 1 MHz modulation frequency for silicon, and the conditions for the one-dimensional treatment are not satisfied. Opsal *et al.* [9] reported that the photoreflectance on a silicon sample increases with increasing modulation frequency when the plasma wavelength is much larger than the probe and pumping beam radii. As a result, they suggested the necessity of three-dimensional treatment for the photoreflectance by including the probe and pumping beam radii.

In this work, we calculated the modulated photoreflectance in silicon by considering the effects of the beam radii of the probe and pumping beam, having

0022–2461

a Gaussian beam profile and modulation frequency. The modulated photoreflectance in a silicon wafer was measured with the same pumping and probe beam radius of about 2 μm in the frequency range 1–100 kHz. The measured magnitude and phase of the photoreflectance were compared with those theoretically calculated.

2. The change of photoreflectance by the generation of plasma and thermal waves

When the energy per photon, $h\nu$, of the incident pumping beam exceeds the band gap energy, E_g, electrons will be excited from the valence band to an energy, $h\nu - E_g$, above the conduction band edge, and holes will be made in the valence band. The electrons above the conduction band and the holes in the valence band are termed photo-excited free carriers. Part of the photon energy of the incident pumping beam generates the photo-excited carrier and the remaining energy is converted to thermal energy. Thermal energy is also generated by the recombination of the photo-excited carriers [6].

When the harmonically modulated pumping beam of a TEM_{00} Gaussian profile with a radius ρ_0 is incident on the surface, the intensity of the pumping beam on the semiconductor, $I(\rho, z, t)$, is given by

$$\begin{aligned} I(\rho, z, t) &= I(\rho)\,e^{-\alpha z}e^{-j\omega t} \\ &= I_{P0}\exp\left[-\frac{\rho^2}{\rho_0^2}\right]e^{-\alpha z}e^{-j\omega t} \end{aligned} \quad (1)$$

where I_{P0} is the maximum intensity at the surface of the specimen, ρ the radial distance from the beam centre, z the depth from the surface, α the absorption coefficient of the pumping beam on the semiconductor, and ω the modulation frequency (Fig. 1).

In previous work, it was assumed that the intensity of the pumping beam within the illuminating region was constant along the radial direction and the photo-excited free carriers and the thermal energy were considered to diffuse into the depth direction from the surface. In this case, the distributions of the photo-excited free carriers and temperature vary with the depth from the surface. However, if the intensity of the pumping beam has a radial distribution, and the photo-excited free carriers and the thermal energy diffuse along the radial direction as well as the depth direction, then the distribution of the photo-excited free carriers and the temperature should be dependent on the beam radius as well as the depth.

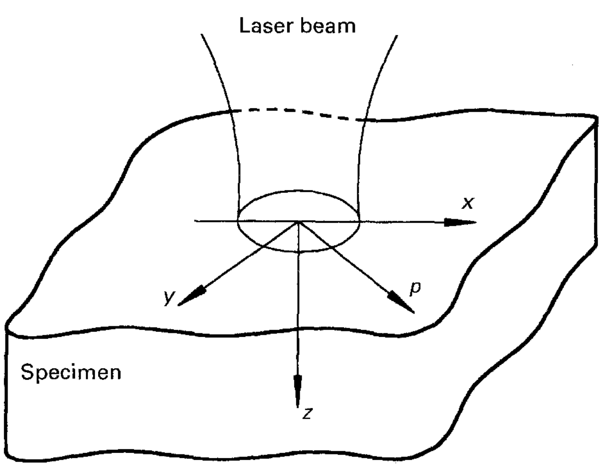

Figure 1 The coordinate system for the calculation of the photoreflectance.

2.1. Change of photoreflectance by the generation of a plasma wave

When the incident pumping beam is modulated with a frequency ω, the number density of photo-excited carriers is given as

$$\Delta N(\rho, z, t) = \Delta N_0(\rho, z)\,e^{-j\omega t} \quad (2)$$

where $\Delta N(\rho, z, t)$ refers to the plasma wave [6]. The diffusion equation of the plasma wave, $\Delta N_0(\rho, z)$, is given by

$$\left(\nabla^2 - \frac{1 - j\omega\tau}{\tau D}\right)\Delta N_0(\rho, z) = \frac{\alpha I(\rho)e^{-\alpha z}}{h\nu D} \quad (3)$$

where τ is the recombination time, D the ambipolar diffusion constant of the semiconductor, and $h\nu$ the energy per photon of the pumping beam.

The Green function of the plasma-wave diffusion equation of Equation 3 is given by

$$\left(\nabla^2 - \frac{1 - j\omega\tau}{\tau D}\right)G_p(\rho, z|\rho', z') = -\frac{1}{2\pi\rho}\delta(\rho - \rho')\delta(z - z') \quad (4)$$

For simplicity of calculation, if the surface recombination is neglected, the boundary condition is

$$D\frac{\partial\Delta N_0(\rho, z)}{\partial z}\bigg|_{z=0} = 0 \quad (5)$$

Using the Green function of the plasma wave of Equation 4 and boundary condition of Equation 5, the plasma wave $\Delta N_0(\rho, z)$ is given as

$$\begin{aligned} \Delta N_0(\rho, z) &= \int_0^\infty 2\pi\rho' d\rho' \int_0^\infty dz' G_p(\rho, z|\rho', z') \times \left(-\frac{\alpha I(\rho')e^{-\alpha z'}}{h\nu D}\right) \\ &= \int_0^\infty \xi d\xi\, J_0(\xi\rho)[A_1(\xi)e^{-\alpha z} \\ &\quad + A_2(\xi)e^{-\sigma_p(\xi)z}]I(\xi) \end{aligned} \quad (6a)$$

where $\sigma_p(\xi) = [\xi^2 + (1 - j\omega\tau)/(\tau D)]^{1/2}$ is the plasma wave vector, $J_0(\xi\rho)$ is the 0th order first-kind Bessel function, and A_1, A_2, and $I(\xi)$ are defined as

$$A_1(\xi) = -\frac{\alpha}{h\nu D[\alpha^2 - \sigma_p^2(\xi)]} \quad (6b)$$

$$A_2(\xi) = -\frac{\alpha}{\sigma_p(\xi)}A_1(\xi) \quad (6c)$$

$$I(\xi) = -\int_0^\infty \rho d\rho\, J_0(\xi\rho)I(\rho)$$

$$= \int_0^{\infty} I_{P0} \exp\left(-\frac{\rho^2}{\rho_0^2}\right) J_0(\xi\rho)\rho d\rho \quad (6d)$$

$$= \frac{I_{P0}\rho_0^2}{2} \exp\left[-\frac{\xi^2\rho_0^2}{4}\right]$$

$$= \frac{P}{2\pi} \exp\left[-\frac{\xi^2\rho_0^2}{4}\right]$$

where $P = (\pi I_{P0}\rho_0^2)$ is the a.c. power of the pumping beam. Thus, the plasma wave, $\Delta N_0(\rho, z)$, generated by the pumping beam, varies with the radial distance, ρ, from the centre of the pumping beam and the depth, z, from the surface. Using the following integration formula

$$\lim_{\rho_0 \to \infty} \int_0^{\infty} \xi d\xi e^{-\frac{\xi^2\rho_0^2}{4}} J_0(\xi\rho) f(\xi)$$

$$= \frac{2}{\rho_0^2} \int_0^{\infty} \delta(\xi) f(\xi) d\xi = \frac{2}{\rho_0^2} f(0) \quad (7)$$

when the pumping beam radius, ρ_0, is infinite, the plasma wave, $\Delta N_0(\rho, z)$ of Equation 6a is rewritten as

$$\Delta N_0(z) = \lim_{\rho_0 \to \infty} \int_0^{\infty} \xi d\xi J_0(\xi\rho) \left(\frac{I_{P0}\rho_0^2}{2} e^{-\frac{\xi^2\rho_0^2}{4}}\right) f(\xi)$$

$$= I_{P0}[A_1(0) e^{-\alpha z} + A_2(0) e^{-\sigma_P(0)z}] \quad (8)$$

where $f(\xi) = [A_1(\xi) e^{-\alpha z} + A_2(\xi) e^{-\sigma_P(\xi)z}]$, $A_1(\xi)$, and $A_2(\xi)$ were defined in Equation 6b and c. The plasma wave, ΔN_0, of Equation 8 is only dependent on the depth, z, and is independent of the radial distance, ρ, which is identical to the one-dimensional results [6, 9, 10].

Assuming that the Drude effect, i.e. the change of refractive index due to the photo-excited carriers, is valid, the photoreflectance due to an electron–hole plasma wave, $\Delta N_0(\rho, z)$, is given as [6, 8]

$$\frac{\Delta R_P}{R_0} = -\frac{2l^2 e^2}{n(n^2-1)m_e c^2} \Delta N_0$$

$$= -C_P \Delta N_0 \quad (9)$$

where R_0 is the reflectance of a probe beam without the pumping beam, l the wavelength of the probe beam, e the electron charge, n the refractive index of the sample for the probe beam, m_e the effective mass of the free carriers, c the velocity of the light, and C_P a constant.

2.2. Change of photoreflectance by the generation of a thermal wave

When the incident pumping beam is harmonically modulated with frequency ω, the temperature variation in the specimen due to the modulated incident pumping beam of frequency ω is given by

$$\Delta T(\rho, z, t) = \Delta T_0(\rho, z) e^{-j\omega t} \quad (10)$$

where $\Delta T(\rho, z, t)$ is called the thermal wave [6]. Because the thermal energy diffuses spatially, the thermal wave diffusion equation is given as

$$\left(\nabla^2 + \frac{j\omega C\rho_d}{K}\right)\Delta T_0(\rho, z) = -\frac{\alpha(h\nu - E_g)I(\rho)e^{-\alpha z}}{h\nu K} - \frac{E_g \Delta N_0(\rho, z)}{\tau K} \quad (11)$$

where ρ_d is the mass density, C the heat capacity, and K the thermal conductivity of a semiconductor. The first term in the right-hand side is the thermal energy induced by part of the absorbed photon energy of the incident pumping beam, which is the excess energy after generating the photo-excited carrier. The second term is the thermal energy induced by recombination of the plasma wave. The Green function of the thermal wave diffusion equation of Equation 11 is given by

$$\left(\nabla^2 + \frac{j\rho_d C\omega}{K}\right) G_T(\rho, z|\rho', z')$$

$$= -\frac{1}{2\pi\rho}\delta(\rho - \rho')\delta(z - z') \quad (12)$$

Ignoring the heat flow into the air, the boundary condition of a thermal wave is

$$\left.\frac{\partial \Delta T_0(\rho, z)}{\partial z}\right|_{z=0} = 0 \quad (13)$$

Using the Green function of the thermal wave of Equation 12 and the boundary condition of Equation 13, the thermal wave $\Delta T_0(\rho, z)$ is given as

$$\Delta T_0(\rho, z) = \int_0^{\infty} 2\pi\rho' d\rho' \int_0^{\infty} dz' G_T(\rho, z|\rho', z') \times \left[-\frac{\alpha(h\nu - E_g)I(\rho')e^{-\alpha z'}}{h\nu K} - \frac{E_g \Delta N_0(\rho', z')}{\tau K}\right]$$

$$= \int_0^{\infty} \xi d\xi J_0(\xi\rho) I(\xi) [A_3(\xi) e^{-\sigma_P(\xi)z} + A_4(\xi) e^{-\alpha z} + A_5(\xi) e^{-\sigma_T(\xi)z}] \quad (14a)$$

where $\sigma_T(\xi) = [\xi^2 - j(\rho_d C\omega)/K]^{1/2}$ is the thermal wave vector, $I(\xi)$ is the same as in Equation 6a, A_3, A_4, and A_5 are defined as

$$A_3(\xi) = [\alpha^2 - \sigma_p^2(\xi)][\sigma_p^2(\xi) - \sigma_T^2(\xi)]\sigma_p(\xi) \quad (14b)$$

$$A_4(\xi) = \frac{\alpha}{\nu K[\alpha^2 - \sigma_T^2(\xi)]}\left\{-(h\nu - E_g) + \frac{E_g}{D\tau[\alpha^2 - \sigma_p^2(\xi)]}\right\} \quad (14c)$$

$$A_5(\xi) = \frac{\sigma_p(\xi)A_3(\xi) + \alpha A_4(\xi)}{\sigma_T(\xi)} \quad (14d)$$

Thus, the thermal wave, $\Delta T_0(\rho, z)$, generated by a Gaussian-form pumping beam, varies with the radial distance, ρ, and the depth, z. Using the same method as in the calculation of the plasma wave, Equation 7, if

TABLE I Values of the parameters used in the calculation

Electron charge, e	4.8×10^{-10}	e.s.u.
Electron mass, m_0	9.1×10^{-28}	g
Effective mass in Si [4, 6], m_e	0.15	m_0
Bandgap energy of Si [12], E_g	1.13	eV
Thermal conductivity of Si [6], K	1.42	$\mathrm{W\,cm^{-1}\,°C^{-1}}$
Refractive index of Si [6], n	3.9	
Absorption coefficient of Si [2, 4], α	10^4	$\mathrm{cm^{-1}}$
Mass density of Si [4], ρ_d	2.33	$\mathrm{g\,cm^{-3}}$
Heat capacity of Si [6], C	0.703	$\mathrm{J\,g^{-1}\,°C^{-1}}$
Ambipolar diffusivity of Si [1, 6], D	20	$\mathrm{cm^2\,s^{-1}}$
Recombination time [1], τ	10^{-4}	s
Temperature coefficient of reflectance [2], C_T	1.5×10^{-4}	$\mathrm{°C^{-1}}$
Wavelength of probe beam (He–Ne laser), l	0.633	µm
Photon energy of pumping beam, (λ = 488 nm Ar + laser), $h\nu$	2.41	eV

the pumping beam radius, ρ_0, is infinite, then the thermal wave, $\Delta T_0(\rho, z)$, is rewritten as

$$\Delta T_0(z) = \lim_{\rho_0 \to \infty} \int_0^\infty \xi \mathrm{d}\xi J_0(\xi\rho)\left(\frac{I_{P0}\rho_0^2}{2} \mathrm{e}^{-\frac{\xi^2\rho_0^2}{4}}\right) g(\xi)$$
$$= I_{P0}\left[A_3(0)\mathrm{e}^{-\sigma_P(0)z} + A_4(0)\mathrm{e}^{-\alpha z} + A_5(0)\,\mathrm{e}^{-\sigma_T(0)z}\right] \quad (15)$$

where $g(\xi) = [A_3(\xi)\mathrm{e}^{-\sigma_P(\xi)z} + A_4(\xi)\mathrm{e}^{-\alpha z} + A_5(\xi) \times \mathrm{e}^{-\sigma_T(\xi)z}]$, $A_3(\xi)$, $A_4(\xi)$, and $A_5(\xi)$ were defined in Equation 14b–d. The thermal wave, $\Delta T_0(z)$, of Equation 15 is only dependent on the depth, z, independent of the radial distance, ρ, and becomes identical to that of the one-dimensional results [6, 10].

Weakiem *et al.* give the temperature dependence of the reflectance up to 200 K above room temperature in silicon as follows [2, 7]

$$\frac{\Delta R_T}{R_0} = C_T \Delta T_0 \quad (16)$$

where C_T is the temperature coefficient of reflectance given in Table I, and R_0 is the reflectance without the pumping beam.

2.3. Calculation of the modulated photoreflectance

The photoreflectance of the semiconductors is affected by both the plasma and thermal waves generated by the modulated incident pumping beam. Thus, the modulated photoreflectance at the surface is given by the summation of these two contributions given by Equations 9 and 16 [6–8]

$$\frac{\Delta R(\rho, t)}{R_0} = \frac{\Delta R_P(\rho, t)}{R_0} + \frac{\Delta R_T(\rho, t)}{R_0}$$
$$= -C_P \Delta N(\rho, 0, t) + C_T \Delta T(\rho, 0, t) \quad (17)$$

where $\Delta R_P(\rho, t)$ and $\Delta R_T(\rho, t)$ are the modulated reflectance components of the thermal and plasma effects, respectively. $\Delta N(\rho, 0, t)$ and $\Delta T(\rho, 0, t)$ are the plasma and thermal waves on the surface, respectively. The photoreflectance oscillates with the same frequency as the modulated pumping beam, ω, and is given by

$$R(\rho, t) = R_0 + \Delta R(\rho, t) = R_0 + \Delta R(\rho)\mathrm{e}^{-j\omega t} \quad (18)$$

then, the intensity of the reflected probe beam is given as follows.

$$\text{Intensity of reflected probe beam} = I_p(\rho) R(\rho, t)$$
$$= I_p(\rho)[R_0 + \Delta R(\rho)\mathrm{e}^{-j\omega t}] \quad (19)$$

where $I_p(\rho)$ is the intensity of the incident probe beam on the semiconductor surface, which is given for the TEM_{00} mode Gaussian beam as

$$I_p(\rho) = I_0 \exp\left(-\frac{\rho^2}{\rho_1^2}\right) \quad (20)$$

where ρ_1, ρ and I_0 are the probe beam radius, the radial distance from the beam centre and the maximum intensity of the probe beam on the surface, respectively. The intensity of the reflected probe beam also oscillates with the modulation frequency, ω, and the power of the reflected probe beam is obtained by integrating the intensity of the reflected probe beam of Equation 19 over the semiconductor surface, S, as follows [1]

Power of reflected probe beam

$$\int_S I_p(\rho) R(\rho, t) \mathrm{d}S$$
$$= \int_S I_p(\rho)\,[R_0 + \Delta R(\rho)\mathrm{e}^{-j\omega t}]\,\mathrm{d}S \quad (21)$$

The power of the reflected probe beam contains a.c. and d.c. components in Equation 21, and we define the modulated photoreflectance, PR, as the ratio of the reflected power of the a.c. and d.c. components,

$$PR = \frac{\text{a.c. power of the reflected probe beam}}{\text{d.c. power of the reflected probe beam}} \quad (22)$$

If both centres of the probe and pumping beams coincide, the a.c. power of the reflected probe beam, the numerator in Equation 22, is

$$\int_0^{2\pi} \mathrm{d}\theta \int_0^\infty \rho \mathrm{d}\rho \Delta R(\rho) I_p(\rho) \quad (23)$$

The d.c. power of the reflected probe beam, the denominator in Equation 22, is

$$\int_0^{2\pi} \mathrm{d}\theta \int_0^\infty \rho \mathrm{d}\rho R_0 I_p(\rho) = \pi \rho_1^2 I_0 R_0 \quad (24)$$

Dividing Equation 23 by Equation 24, we obtain the PR of Equation 22 as

$$PR = \frac{1}{\pi \rho_1^2} \int_0^{2\pi} d\theta \int_0^{\infty} \rho d\rho \left\{ e^{-\rho^2/\rho_1^2} \left[\frac{\Delta R(\rho)}{R_0} \right] \right\} \quad (25)$$

By substituting the modulated photoreflectance of Equation 17 into Equation 25, PR is rewritten in terms of the thermal and plasma waves as follows

$$PR = \frac{2}{\rho_1^2} \int_0^{\infty} \rho d\rho \left(\exp - \frac{\rho^2}{\rho_1^2} \right) [- C_P \Delta N_0(\rho, 0) + C_T \Delta T_0(\rho, 0)] \quad (26a)$$

The absorption coefficient of the incident pumping beam of an Ar^+ laser is about 10^4 cm^{-1} in a silicon wafer [2], then, the incident pumping beam will be absorbed in ~ 1 μm range of the subsurface. Therefore, we assume that the absorption coefficient, α, is infinite, and by substituting $\Delta N_0(\rho, 0)$ of the plasma wave of Equation 6 and $\Delta T_0(\rho, 0)$ of the thermal wave of Equation 14 into PR of Equation 26a, using the following integration formula

$$\int_0^{\infty} e^{-\rho^2/\rho_1^2} J_0(\xi\rho) \rho d\rho = \frac{\rho_1^2}{2} \exp\left(- \frac{\xi^2 \rho_1^2}{4} \right) \quad (26b)$$

the PR is obtained as follows

$$PR_{3D} = \frac{P}{2\pi} \int_0^{\infty} \xi d\xi e^{-\xi^2 \rho_e^2/2} \left\{ - \frac{C_P}{D\sigma_p(\xi) h\nu} + \frac{C_T}{K\sigma_T(\xi)} \times \left(1 - \frac{E_g}{h\nu} \right) + \frac{C_T}{KD\tau[\sigma_p^2(\xi) - \sigma_T^2(\xi)]} \frac{E_g}{h\nu} \times \left(\frac{1}{\sigma_T(\xi)} - \frac{1}{\sigma_p(\xi)} \right) \right\} \quad (27)$$

where $\rho_e = [(\rho_1^2 + \rho_0^2)/2]^{1/2}$ is called the effective beam radius.

The photoreflectance, PR_{3D}, as seen in Equation 27, depends on the radii of the probe and pumping beams ρ_1 and ρ_0, and we assign Equation 27 as the three-dimensional PR.

In previous works, however, the effects of pumping and probe beam size on PR have not been considered [6–11]. Under the conditions in which the radii of the probe and/or the pumping beam, ρ_1 and ρ_0, are larger than the wavelength of the plasma wave and the thermal wave, i.e. $\rho_1/\lambda_p \gg 1$, $\rho_1/\lambda_T \gg 1$, $|\rho_0/\lambda_p \gg 1$, $\rho_0/\lambda_T \gg 1$, then Equation 27 is approximated as

$$PR_{1D} \approx \frac{P}{\pi \rho_e^2} \left\{ - \frac{C_P}{D\sigma_p(0) h\nu} + \frac{C_T}{K\sigma_T(0)} \left(1 - \frac{E_g}{h\nu} \right) + \frac{C_T}{KD\tau[\sigma_p^2(0) - \sigma_T^2(0)]} \times \frac{E_g}{h\nu} \left[\frac{1}{\sigma_T(0)} - \frac{1}{\sigma_p(0)} \right] \right\} \quad (28)$$

where, $\sigma_T(0)$ and $\sigma_p(0)$ are the thermal and plasma wave vectors in one-dimension and three-dimensions, respectively. The wave vector, wavelength and modulation frequency are related by

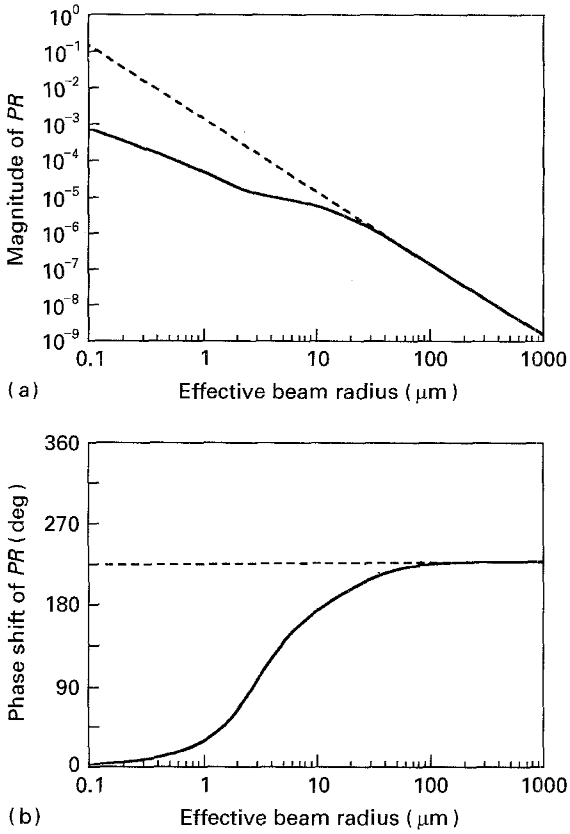

Figure 2 (a) Variation of the magnitude, and (b) phase of the calculated photoreflectance with the effective beam radius in a silicon wafer. (---) one-dimensional analysis, (———) three-dimensional analysis. Modulation frequency = 1 MHz, $D = 20$ cm^2 s^{-1}, $\tau = 100$ μm.

$$\lambda_p = \frac{2\pi}{|\sigma_p(0)|} = 2\pi[(\tau D)/|(1 - j\omega\tau)|]^{1/2} \quad (29a)$$

$$\lambda_T = \frac{2\pi}{|\sigma_T(0)|} = 2\pi[K/(\rho_d C\omega)]^{1/2} \quad (29b)$$

The result of Equation 28 agrees with the one-dimensional PR obtained by Opsal *et al.* [6]. Thus, we assign PR_{1D} of Equation 28 to be the one-dimensional photoreflectance.

3. Results and discussion

We assumed that the power of the pumping beam in the silicon wafer was 1 mW and the radii of probe and pumping beams were the same in the calculation, for simplicity ($\rho_e = [(\rho_1^2 + \rho_0^2)/2]^{1/2}$ and $\rho_1 = \rho_0$, then $\rho_e = \rho_1$ and $\rho_e = \rho_0$). The magnitude and phase of PR_{1D} and PR_{3D} were calculated from Equations 28 and 27, respectively, using the parameters listed in Table I.

3.1. The variation of photoreflectance with effective beam radius

Fig. 2a shows the variations of the magnitude of PR_{1D} and PR_{3D} with the effective beam radius at 1 MHz modulation frequency in which the dashed and solid lines represent the magnitude of the calculated PR_{1D}

and PR_{3D}, respectively. The PR_{1D} decreases as the inverse square of the effective beam radius, ρ_e, in agreement with Equation 28 in the whole range. PR_{3D} is about 100 times less than PR_{1D} for the effective beam radius 0.1 μm and decreases with the effective beam radius, ρ_e, until 112 μm, followed by the same dependence on ρ_e as for the one-dimensional case. The wavelengths of the thermal and plasma waves are given by $\lambda_T = 46.7$ μm and $\lambda_p = 112$ μm, respectively, for the 1 MHz modulation frequency of the incident pumping beam from Equation 29. So, $\rho_e/\lambda_T > 2.36$ and $\rho_e/\lambda_p > 1$, and the necessary condition, $\rho_e/\lambda_T > 1$ and $\rho_e/\lambda_p > 1$, for PR_{3D} to be equal to PR_{1D} is satisfied when the effective beam radius, ρ_e, is larger than 112 μm. For $\rho_e < 112$ μm, in turn $\rho_e < \lambda_p$ ($= 112$ μm at 1 MHz modulation frequency), then $\rho_e/\lambda_p < 1$ and the aforementioned conditions for PR_{1D} to be equal to PR_{3D} are not satisfied; consequently, the magnitude of PR_{3D} becomes smaller than that of PR_{1D} due to the energy loss within the effective beam radius.

Fig. 2b shows the variation of the phase shift of PR_{1D} and PR_{3D} with the effective beam radius at 1 MHz modulation frequency. The dashed line, the phase shift of PR_{1D}, is nearly constant at 225°, whereas the solid line, the phase shift of PR_{3D}, increases with the effective beam radius, reaching the same constant value of PR_{1D} at the beam radius of 112 μm caused by the same reason as the variation of the magnitude in Fig. 2a.

3.2. The variation of photoreflectance with modulation frequency

The experimental equipment used for the PR measurement is shown in Fig. 3. An acousto-optic modulator and function generator were used for the modulation of the pumping beam of an Ar^+ laser ($\lambda = 488$ nm, 15 mW). The He–Ne laser ($\lambda = 632.8$ nm, 5 mW) was used as a probe beam and the changes in the reflectivity of the He–Ne laser beam were measured with a silicon photodiode detector, filtered by a 632.8 nm bandpass interference filter. The output voltage of the detector was measured via a lock-in amplifier (SR 530) controlled by a personal computer through GPIB.

Fig. 4a is the modulation frequency dependence of the PR for the effective beam radius of 2 μm. The solid and dashed lines represent the magnitude of PR_{1D} and PR_{3D}, respectively and the circles represent the measured PR data for a bare silicon p-type (1 0 0) wafer with a resistivity of 20 Ω cm. The magnitude of PR_{3D} is nearly constant in the frequency range between 1 kHz and 10 MHz, whereas that of PR_{1D} decreases with the modulation frequency as $\omega^{-1/2}$, in the same manner as in Fig. 3a and b of Vitkin *et al.* [8]. The magnitude of PR_{1D} approaches that of PR_{3D} as the modulation frequency increases. The wavelengths of thermal and plasma waves are $\lambda_T = 1476$ μm and $\lambda_p = 2531$ μm for the 1 kHz modulation frequency, $\lambda_T = 14.7$ μm and $\lambda_p = 35.45$ μm for the 10 MHz modulation frequency, respectively. For the effective beam radius, $\rho_e = 2$ μm, $\rho_e/\lambda_T = 0.001\,36$ and $\rho_e/\lambda_p = 0.000\,79$ for the 1 kHz modulation frequency, and $\rho_e/\lambda_T = 0.136$ and $\rho_e/\lambda_p = 0.0564$ for the 10 MHz modulation frequency, respectively. Thus, ρ_e/λ_T and ρ_e/λ_p approach 1 as the modulation frequency increases from 1 kHz to 10 MHz, because the thermal and plasma wavelengths decrease with increase of modulation frequency, as in

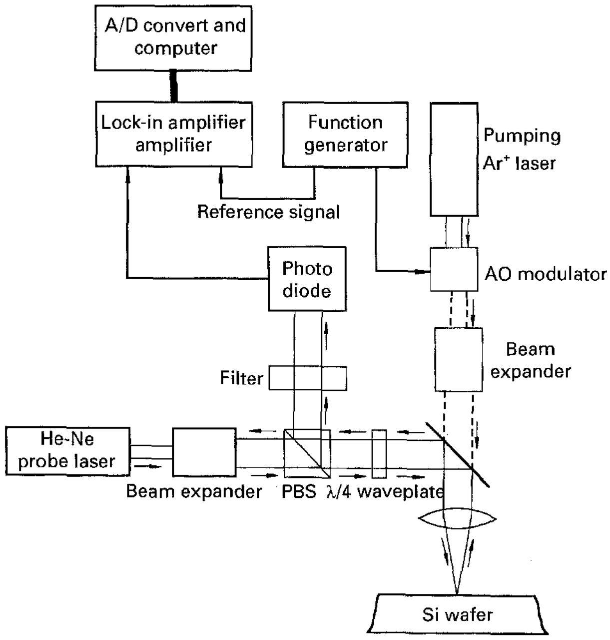

Figure 3 A schematic diagram of the experimental equipment for the measurement of photoreflectance.

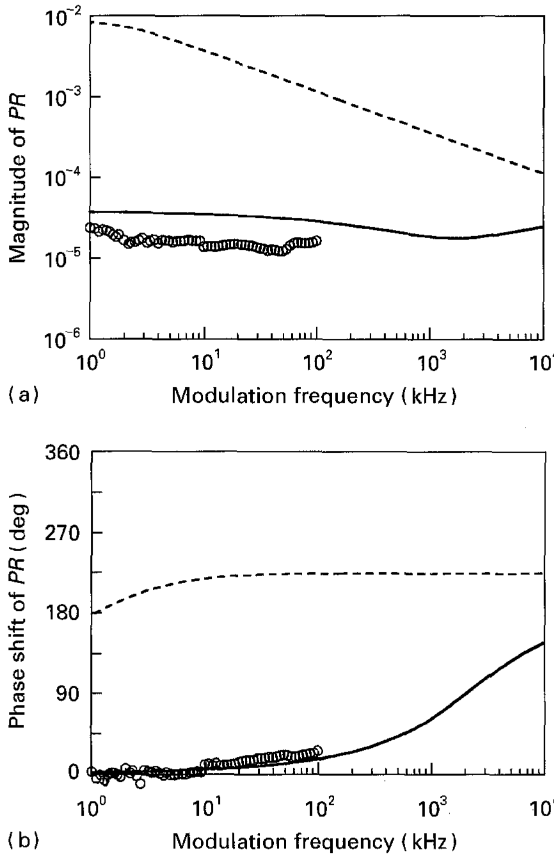

Figure 4 (a) Variation of the magnitude, and (b) phase of the calculated and measured photoreflectance with the modulation frequency in a silicon wafer. (---) One-dimensional analysis, (——) three-dimensional analysis. (○) Experimental data (effective beam radius $= 2$ μm, $D = 20$ cm^2 s^{-1}, $\tau = 100$ μm).

Equation 29, consequently, PR_{3D} approaches PR_{1D} by satisfying the equivalence conditions. The smaller magnitude of PR_{3D} compared to that of PR_{1D} over the whole frequency range is caused by the energy loss within the effective beam radius due to not satisfying the equivalence conditions. The agreement between the variation of calculated and measured magnitudes of PR in the limited modulation frequency range suggests justification for the three-dimensional PR analysis.

In Fig. 4b, the solid and dashed lines depict the variation of phase in PR_{1D} and PR_{3D}, with the modulation frequency, respectively, and the circles represent the measured phase data of the output in the lock-in amplifier. The phase shift of PR_{1D} varies from 180° to 225° with modulation frequency, but that of PR_{3D} increases from 0° at near 1 kHz and approaches that of PR_{1D}. The good agreement between the measured and calculated phase shifts confirms again the justification of the three-dimensional analysis to account for the observed phase shift, as in the case of the variation of the magnitude of PR in Fig. 4a.

4. Conclusion

The effects of beam size and modulation frequency on photoreflectance were investigated for a silicon wafer by considering the generation and propagation of plasma and thermal waves. The photoreflectance, when considering one-dimensional generation and propagation of plasma and thermal waves, PR_{1D}, at 1 MHz modulation frequency, decreased as the inverse square of the effective beam radius, ρ_e. However, the photoreflectance when considering three-dimensional generation and propagation, PR_{3D}, was 100 times smaller than PR_{1D} at $\rho_e = 0.1$ μm, and decreased with ρ_e, followed by the same variation as PR_{1D} from $\rho_e = 112$ μm. Theoretical analysis confirmed that the equivalence conditions of $\rho_e/\lambda_p > 1$ and $\rho_e/\lambda_T > 1$ for $PR_{1D} = PR_{3D}$ were satisfied when $\rho_e > 112$ μm. However, for $\rho_e < 112$ μm, the equivalence conditions were not satisfied; consequently, PR_{3D} becomes less than PR_{1D} due to the energy loss within the effective beam radius. The phase shift of PR_{1D}, was nearly constant at 225°, whereas that of PR_{3D} increased with the effective beam radius, reaching the constant value of PR_{1D} at the beam radius 112 μm. The approach of the phase shift of PR_{3D} to that of PR_{1D} was caused by the same reason as the variation of the magnitude of PR.

PR_{3D} was nearly constant in the frequency range between 1 kHz and 10 MHz, whereas PR_{1D} decreased with the modulation frequency as $\omega^{-1/2}$, approaching PR_{3D}. As the modulation frequency increased from 1 kHz to 10 MHz, the wavelengths of thermal and plasma waves approached the effective beam radius, ρ_e/λ_T and ρ_e/λ_p approaching 1; consequently, the magnitude of PR_{3D} approached that of PR_{1D}. The magnitude of PR_{3D} was smaller than that of PR_{1D} in the whole frequency range, due to the energy loss within the effective beam radius. The agreement between the variation of the calculated and measured magnitude of PR for a silicon wafer with the modulation frequency suggests the justification of the three-dimensional PR analysis. The phase shift of PR_{1D} varied from 180° to 225° with increase of the modulation frequency of the incident pumping beam, but that of PR_{3D} increased from 0° at ~1 kHz and approached that of PR_{1D}. The good agreement between the measured and calculated phase shift justified again the three-dimensional analysis to account for the observed phase shift, as in the case of the variation of the magnitude of PR with the modulation frequency.

References

1. D. GUIDOTTI and H. M. van DRIEL, *Appl. Phys. Lett.* **47** (1985) 1336.
2. H. A. WEAKIEM and D. REDFIELD, *J. Appl. Phys.* **50** (1979) 1491.
3. N. G. NILLSSON, *Solid State Commun.* **7** (1969) 479.
4. L.-A. LOMPRE, J.-M. LIU, H. KURZ and N. BLOEMBERGEN, *Appl. Phys. Lett.* **44** (1984) 3.
5. A. M. BONCH-BRUEVICH, V. P. KOVALEV, G. S. ROANOV, YA. A. IMAS and M. N. LIBENSON, *Sov. Phys. Tech. Phys.* **13** (1968) 507.
6. J. OPSAL and A. ROSENCWAIG, *Appl. Phys. Lett.* **47** (1985) 498.
7. C. CHRISTANTINOS, I. A. VITKIN and A. MANDELEIS, *J. Appl. Phys.* **67** (1990) 2815.
8. I. A. VITKIN, C. CHRISTOFIEDS and A. MANDELEIS, *ibid.* **67** (1990) 2822.
9. J. OPSAL, M.W. TAYLOR, W. L. SMITH and A. ROSENCWAIG, *ibid.* **61** (1987) 240.
10. D. FOURNIER, C. BOCCARA, A. SKUMANICH and NABIL M. AMER, *ibid.* **59** (1986) 787.
11. J. OPSAL, A. ROSENCWAIG and D. L. WILLENBORG, *Appl. Opt.* **22** (1983) 3169.
12. D. J. DUNSTAN, in "Properties of Silicon" (INSPEC, 1988) p. 171.

Received 29 November
and accepted 13 December 1994